Moisture content of the coating determines the water permeability as measured by 1D magnetic resonance imaging

Progress in Organic Coatings 130 (2019) 114–123

Contents lists available at ScienceDirect

Progress in Organic Coatings

journal homepage: www.elsevier.com/locate/porgcoat

Moisture content of the coating determines the water permeability as measured by 1D magnetic resonance imaging

Özlem Gezici-Koç[a], Sebastiaan J.F. Erich[a,b,*], Hendrik P. Huinink[a], Leendert G.J. van der Ven[a], Olaf C.G. Adan[a,b]

[a] Department of Applied Physics, Eindhoven University of Technology, P.O. Box 513, 5600 MB, Eindhoven, the Netherlands
[b] TNO, The Netherlands Organization for Applied Scientific Research, P.O. Box 49, 2600 AA, Delft, the Netherlands

ARTICLE INFO

Keywords:
Wood
Coatings
NMR imaging
Water uptake
Permeability

ABSTRACT

In addition to the desired aesthetical properties, a coating is applied to protect against weathering. A coating prevents moisture accumulation in wood by reducing the water uptake into the wood by its barrier function. The studies in the coating permeability has gained interest with the shift towards waterborne coatings, which make coatings intrinsically more sensitive to water. This paper presents the results of a Nuclear Magnetic Resonance (NMR) Imaging study on the influence of a coating`s moisture content on the permeability of a coating on wood. In this work, pine sapwood, oak, and teak were selected as wood types covering a whole range of low to high density wood types. Three transparent coatings were formulated: a solventborne alkyd, a waterborne alkyd and a waterborne acrylic. The aim of this study is to investigate how sensitive the permeability of coatings on wood against moisture during liquid water uptake and subsequent drying below Fiber Saturation Point. During both water uptake and subsequent drying, the coating limited transport was observed for the studied wood-coating combinations. The NMR profiles are used to calculate the water permeability of coatings on wood. We have demonstrated the direct relation of the permeability with the average water activity inside the coating, which is connected to the activities of both sides of the coating. We observed reasonably well correlation between the sorption isotherm of the coatings and the permeability, which indicates that the permeability variations are due to the amount of water present in the coating. Finally, we have shown that the permeability is not about the type of water vapour or liquid present at one side of the coating, it is all about the local moisture content in the coating.

1. Introduction

Wood is a porous material that can accumulate moisture. If the moisture content of the wood exceeds Fiber Saturation Point (FSP) - the point where a transition occurs from a regime of only bound water towards a regime of free and bound water together [1] - it may result in favourable conditions for decay. For protective and decorative reasons, coatings are generally applied on wooden substrates. The regulations concerning the usage and emissions of volatile organic compounds (VOCs) have led to increased use of waterborne (WB) coatings. While solventborne (SB) coatings are still have their place, WB coatings are becoming more and more common in the wood coatings sector. WB coatings are more sensitive to water compared to SB coatings [2], which requires more understanding of the influence of coatings on the changes of wood moisture content.

Several approaches have been used to understand the influence of coatings on water transport through coated wood and resulting wood moisture content. For example, the average moisture content in bulk wood was measured to investigate the water transport properties through coatings [2–4]. However, the inhomogeneous distribution of water close to the surface have been demonstrated by many studies [5–8]. These findings reveal the need of measuring the moisture content with spatial and time resolution to evaluate the barrier properties of coatings.

Nuclear Magnetic Resonance (NMR) imaging is one of the methods to study wood moisture content, which is non-destructively providing temporally and spatially resolved moisture profiles [9]. It has proven to be an excellent tool for determining the moisture content of wood samples during water sorption [7,10–12]. The second advantage of NMR imaging compared to other methods (such as weighing [13,14] or X-ray computer tomography (CT) [15] or neutron imaging [16]/ radiography [17]) is its ability to distinguish the state of moisture as

* Corresponding author at: Department of Applied Physics, Eindhoven University of Technology, P.O. Box 513, 5600 MB, Eindhoven, the Netherlands.
E-mail address: s.j.f.erich@tue.nl (S.J.F. Erich).

https://doi.org/10.1016/j.porgcoat.2019.01.043
Received 10 September 2018; Received in revised form 14 January 2019; Accepted 22 January 2019

bound or free water. It allows understanding the transport properties by understanding the changes in bound and free water [18].

Recently, we have published a study, which aimed to elucidate the influence of the wooden substrate on the water vapour permeability of the coating applied to it [11]. NMR imaging was used to measure the moisture content distribution and quantify the changes in bound and free water in wood (pine sapwood, teak and oak) as a function of coating permeability (SB alkyd, WB alkyd and WB acrylic) during drying of completely water saturated samples. We observed that water transport appeared to be externally (i.e. coating) limited for all studied wood-coating combinations. We furthermore compared water vapour permeability of free films and wood supported films to understand the influence of the wood-coating interactions. We found that the interaction of the coating with the wood has no influence on the water vapour permeability for the considered combinations.

The dependence of the permeability to the physical state of water is still in debate [19,20]. In principle, there is no theoretical difference between the permeation of liquid and water vapour for non-porous materials [21,22]. However, the coatings have porous structure and the transport of water may occur through capillary flow (especially in pigmented coatings) that may result in the differences between liquid water and water vapour permeability [21–23]. It is often believed that the permeability of liquid water is higher than water vapour permeability [20]. Moreover, it is also known that the moisture absorption – both from liquid and gaseous state of water – strongly influences the properties of many polymeric materials [24]. For most of the acrylic films, the clusters of surfactant in the film acts as water reservoir, and is hydrated by water. Increasing the amount of water enlarges the hydrated domains leading to scatter light, thus it loses transparency and turns into white upon water absorption. It regains transparency upon drying above its T_g. Additionally, exposure to liquid water causes continuous addition of water to the hydrated domains and results in considerable swelling of the surrounding polymer. This may influence film properties irreversibly and leave large voids behind [24,25]. These voids may act as water channels and influence water permeability. However, it is still under investigation whether or not water vapour permeability during drying is really different than liquid water permeability during water uptake.

The aim of this study is to investigate how sensitive the permeability of coatings on wood against moisture during long term exposure (about 3 months) to liquid water and subsequent drying below FSP. Various combinations of wood and coating types are studied that same wood (pine sapwood, teak and oak) and coating (SB alkyd, WB alkyd and WB acrylic) types with the previous study [11] are used. More specifically, four subsequent steps are taken to answer to this objective. The first step is to measure the moisture content (MC) distribution in coated wood during liquid water uptake. Besides the MC profiles, relaxation analysis is used to identify and quantify the state of water during water uptake. The second step is to measure the MC distribution during subsequent drying on the same samples. In the third step, the average moisture content in coated wood is used for permeability calculations. Finally, the permeability results are correlated with the average water activity in the coating, and the sorption isotherms of the coatings.

2. Materials and methods

2.1. Wood and coating types

Three types of wood were studied: one type of softwood, pine sapwood (*Pinus sylvestris*), and two types of hardwood, oak (*Quercus petraea*) and teak (*Tectona grandis*). The properties of these wood types were given in detail in our previous work [10], and summarized in Table 1. The sorption isotherms are recalled in Fig. 1.

Two types of WB coating and one SB coating as a reference were studied to gain knowledge of how coatings resist water. Three transparent coating formulations, WB acrylic, WB alkyd, and SB alkyd, were prepared by AkzoNobel Decorative Paints, Sassenheim, the Netherlands, specifically for this work, which is a part of a previous work [11]. The WB acrylic dispersion was based on butyl acrylate and methyl methacrylate, with a glass transition temperature (T_g) of 2.4 °C and a minimum film formation temperature of 7 °C. The final WB acrylic composition had a solid content of 35 wt. (weight) %, and the surfactant amount of 6.9 wt.% on solid content. The alkyd binder for both WB and SB compositions was based on tall-oil fatty acids with a long oil length and low molecular weight. The WB alkyd emulsion was prepared using a 2% load of non-ionic surfactant to obtain an average particle size of 200 nm. The final WB alkyd composition had a solid content of 35 wt.%, and the surfactant amount of 5.1 wt.% on solid content. The final SB alkyd formulation had a solid content of 65 wt.%.

2.2. Coatings on wood

The coatings (WB Acrylic, WB alkyd, SB alkyd) were applied by brush on wood (pine sapwood, oak, and teak). The overview of studied wood-coating combinations is given in Table 1.

In all combinations, three layers were applied to get a final effective thickness of around 50 µm on wood. The first layer was sanded to eliminate surface roughness. Two more subsequent layers were applied. The time between the applications of consecutive layers was one day. The coated wood samples were dried at room condition, i.e. 21 °C and 40% relative humidity, for at least four months before the measurements were performed.

The dry film thickness of coatings on wood was determined from the cross-sections of the samples by using light microscope (Leica DMRX) according to ISO 2808:2007 [26] and ISO 1463:2003 [27], shown in Fig. 2.

Firstly, 20 mm diameter cylindrical samples were drilled from 10 mm thick coated wood panels. The samples were fixed on a small piece of wood with epoxy glue for better handling. The cross-sections were made with a sledge microtome by cross cutting them with a sharp microtome knife. The cross-sections were examined with a light microscope using UV-light, where the investigated length was approximately 12 mm. The thickness analysis was based on measuring 10 different points for each sample. Thickness analyses were performed on the same samples which were used for the NMR experiments.

2.3. NMR imaging and relaxometry

2.3.1. Principles and settings

As in the previous work [11], NMR imaging and relaxometry was used to measure the moisture content distribution and to quantify the changes in bound and free water in coated wood. For details of the NMR principles we refer to our previous papers [10,11].

The experiments were performed with a home-built NMR set-up with a main magnetic field of 0.75 T and a constant gradient of 418 m T/m. It was designed with an electromagnet from GMW (Model 3473-70) and RadioProcessor™ (USB board) from SpinCore as a digital system for RF signal acquisition, detection and processing [11].

The moisture profiles were obtained with a Hahn Spin Echo (HSE) sequence and a Carr-Purcell-Meiboom-Gill (CPMG) sequence was used to measure the relaxation time, T_2.

The resulting NMR signal shows an exponential decay, as described by:

$$I(\tau) = \sum_{i=1}^{m} I_i \, exp\left(-n \cdot 2\tau / T_2^i\right) \quad (1)$$

where $I(\tau)$ is the observed NMR signal at a time, I_i is the signal from each exponential component, and m is the number of components. The signal intensity of each exponential term is proportional to the pore volume [28,29]. Therefore, the signal intensity of each term versus T_2 values produces a continuous spectrum of T_2 values, i.e. a map of the

Table 1
Overview of studied wood-coating combinations.

Wood			Applied coating	
Type	Density (kg/dm^3)	Structure	Type	Direction
Pine sapwood (*Pinus sylvestris*)	~ 0.54	No vessels	SB alkyd WB alkyd WB Acrylic	Radial plane: the rays are parallel and the growth rings are perpendicular to the coated surface
Teak (*Tectona grandis*)	~ 0.64	Ring porous	SB alkyd WB alkyd WB Acrylic	Tangential plane: the growth rings and rays are oriented diagonally (about 45 ° angle) to the coated surface
Oak (*Quercus petraea*)	~ 0.64	Semi-ring porous	SB alkyd WB alkyd WB Acrylic	Tangential plane: the rays are perpendicular and the growth rings are parallel to the coated surface, i.e. vessels are oriented parallel to the surface

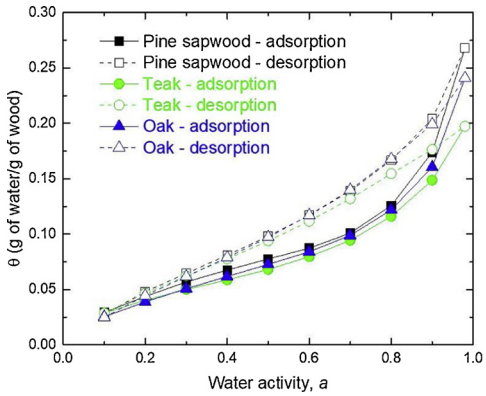

Fig. 1. Sorption isotherms for pine sapwood, oak and teak measured by Dynamic Vapour Sorption (DVS) at 25 °C. The data is obtained from our previous study [10].

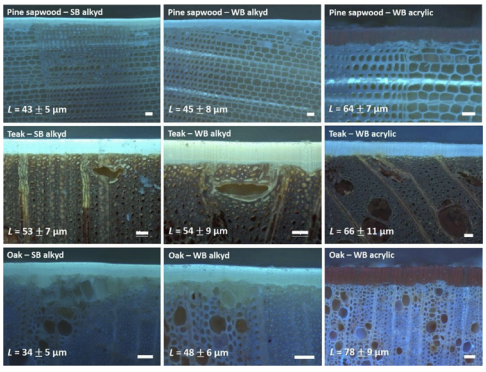

Fig. 2. The light microscope images of the cross-sections of coated wood using UV-light. The scale bar in the corners represent 50 µm. The thickness analysis is based on 10 different points. The average values (AV) and the standard deviation (SD), L = AV ± SD, are given in the corners of each cross section images.

volume occupied by each pore size or the pore size distribution. For details of the method of T_2 relaxation analysis we refer to our previous papers [10,11].

The settings are summarized in Table 2. t_e is the echo time, t_{ww} is the recording window, t_{90° is the pulse time, G_z is the linear magnetic field gradient, Δx is the theoretical spatial resolution, n is the number of echoes, n_{avg} is the number of signal averages, and t_{RT} is the repetition time between two subsequent pulses.

In order to determine the local hydrogen density, the measured signal profiles were divided by the signal profile of a reference sample (an equal volume of aqueous 0.01 M $CuSO_4$ solution).

Table 2
The measurement settings of Hahn Spin Echo (HSE) and Carr-Purcell-Meiboom-Gill (CPMG) pulse sequences used for water uptake and subsequent drying of coated wood for all studied wood-coating combinations.

	t_e (µs)	t_{ww} (µs)	t_{90° (µs)	G_z (mT/m)	Δx (mm)	n	n_{avg}	t_{RT} (s)
HSE	200	120	25	418	0.46	–	4	8
CPMG	200	120	25	418	0.46	2048	32	8

The moisture content (MC) was determined from the measured NMR signal based on calibration done in our previous study [10] and expressed as a percentage of the mass of water over the mass of dry wood (θ). The mass of dry wood is 1.7 ± 0.04 g for pine sapwood, 2.0 ± 0.04 g for oak and 2.0 ± 0.02 g for teak [10].

2.3.2. Samples and sample holder for water uptake/drying of coated wood

20 mm diameter cylindrical samples were drilled from 10 mm thick wood panels (radial cut for pine sapwood, and tangential cut for oak and teak). Prior to the water uptake measurements, all samples were equilibrated at 33% RH for at least 4 weeks. The cylindrical wood samples were mounted in Teflon sample holders. These holders do not show any ^{1}H NMR signal. A glass tube was glued on top of the samples to act as a water reservoir, as shown in Fig. 3. The glued glass tube reduces the effective surface radius of the samples to 6.5 ± 0.5 mm from 10 mm. Note that the lateral distribution is so fast that this has no influence on the water distribution. The sides of the samples were sealed with Teflon grease and Teflon tape to ensure that water can only enter the wood from the top side. Distilled water was put on top of coated wood samples.

The same samples used for the water uptake were used for subsequent drying. After completing the long term (about 100 days) water uptake, the remaining liquid water was taken away from the top of the samples and the top surface was exposed to a flow of dry air. The air flow was set at 3 L/min with an RH about 0–5% at room temperature (~22 °C).

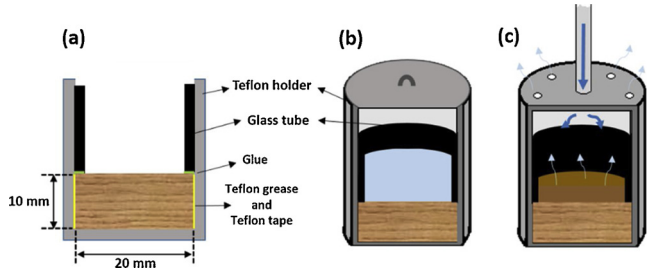

Fig. 3. (a) Schematic of the inner structure of the sample holder. An illustration of the sample holder (b) for water uptake, and (c) for subsequent drying showing the air flow inside.

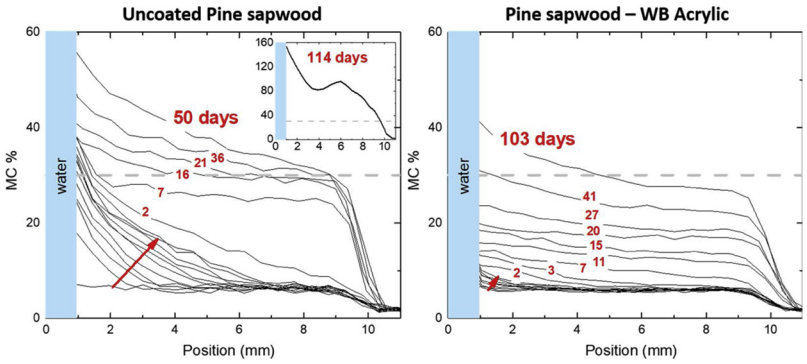

Fig. 4. The moisture content (MC) profiles of water uptake of uncoated and WB acrylic coated pine sapwood. The data for uncoated pine sapwood is obtained from our previous study [10]. Profiles were obtained every 2 h during the first day represented by an arrow, then at indicated times in terms of days.

3. Results and discussion

3.1. Water uptake

3.1.1. Uncoated wood versus coated wood

In order to understand barrier properties of coatings during long term exposure to liquid water uptake, we first compare uncoated and coated wood. As an example of comparison, uncoated and WB acrylic coated pine sapwood were chosen that the moisture content (MC) profiles during water uptake are given in Fig. 4. In our previous paper we discussed water transport properties in uncoated wood during water uptake [10], which we will use as a reference in this study. The surface exposed to liquid water is located at position $x = 0$. The FSP is indicated by the horizontal dashed line, which was found to be around a MC of 29% for pine sapwood by DVS [10]. In comparison with the literature values, this FSP value is close to the value obtained by NMR method, which is reported as 35 ± 4% for pine sapwood [30]. However, as discussed by Hill et al. [31], the solute exclusion method – supposed to measure the total water capacity of the cell wall – may result FSP values above 40%. The differences in FSP by these methods are considered to be due to incomplete wetting of the lignocellulosic material when absorbing moisture from the initial dry state [31].

For uncoated wood, three phases of water uptake are observed. Firstly, during the early phase of the uptake (first 2 days), a front develops indicating that the transport is internally limited. This front occurs until the moisture reaches the bottom, where the MC remains below the FSP. Secondly, there is a homogeneous increase up to the FSP (between 7 and 16 days). Thirdly, the last phase of water uptake occurs above the FSP (between 21 and 114 days), where the MC significantly exceeds the FSP. In the case of WB acrylic coated pine sapwood, we observe the first phase of the uptake during the first week, where the front is not as visible as in the case of uncoated wood. The second phase of homogeneously increasing profiles up to the FSP is observed until around 40 days. Even after about 100 days exposure to liquid water, the MC of the upper part of the sample is slightly higher than the FSP, and the MC of the bottom part is close to but lower than the FSP. In other words, the third phase of the uptake above the FSP is hardly visible for coated wood.

3.1.2. Combinations of wood and coatings types

The barrier properties of wood coatings against moisture are investigated by studying various combinations of wood and coating types during long term exposure to liquid water, of which the moisture content profiles are given in Fig. 5. Note that the FSP was found to be around a MC of 30% for oak and 22% for teak [10].

4. Pine sapwood

For SB alkyd and WB alkyd coated pine sapwood, the first two phases of the uptake are similar as in the case of WB acrylic coated pine sapwood. The first phase of the uptake is observed during the first week, where the front is not much obvious. Then until around 40 days, the second phase of homogeneously increasing profiles up to the FSP is observed. Until around 100 days, the third phase of the uptake exceeding the FSP is observed for WB alkyd coated pine sapwood, while it is hardly visible for the others.

4.1. Teak

For teak with 3 different coating types (SB alkyd, WB alkyd and WB acrylic), the first phase of the uptake is observed during the first week, where the front is not much obvious. The second phase of homogeneously increasing profiles up to the FSP is observed until 40 days for SB alkyd and WB acrylic coated teak, and until 20 days for WB alkyd coated teak. The third phase of the uptake exceeding the FSP is clearly observed for SB alkyd and WB alkyd coated teak until 120 days, while it is hardly visible for WB acrylic coated teak even after about 100 days.

4.2. Oak

In the case of oak, the wave-like moisture distribution is observed for SB alkyd, WB alkyd and WB acrylic coated oak. This is because of the structure of the wood, i.e. the orientation of the vessels to the surface [32]. The vessels in the earlywood rings have different water capacity compared to the cells in the latewood rings. When these vessels are oriented parallel to the surface as in this case, a lower MC is observed in these regions, which leads wave-like moisture distribution through wood samples. For oak with 3 different coating types (SB alkyd, WB alkyd and WB acrylic) we again observe the first phase of front like uptake for the first week. For SB alkyd and WB alkyd coated oak, the second phase of homogeneously increasing profiles up to the FSP is observed until 22 days. The third phase is observed until 95 days, where the MC exceeds the FSP over the whole sample. For WB acrylic coated oak, the third phase is not observed at all. Even after 93 days the MC is far below the FSP – around 20% – all over the sample, even close to the surface.

Besides the MC profiles, relaxation analysis is used to identify and quantify the state of water during water uptake, shown in Fig. 6. The relaxation analysis is performed at three different points, around 2 mm (top), 5 mm (middle) and 8 mm (bottom) below the coated surface, where it relates to a region of 0.5 mm width at each position.

At all positions, free water is only observed after all the cell walls are saturated with bound water. This is the transition point from the second phase of the uptake to the third phase. The number of days indicated by vertical arrows represent the beginning time of the third phase. During the first and the second phases of the uptake below FSP, only bound water is available showing the transport in the vapour phase and in the wood fibers [10]. Free water is available only in the

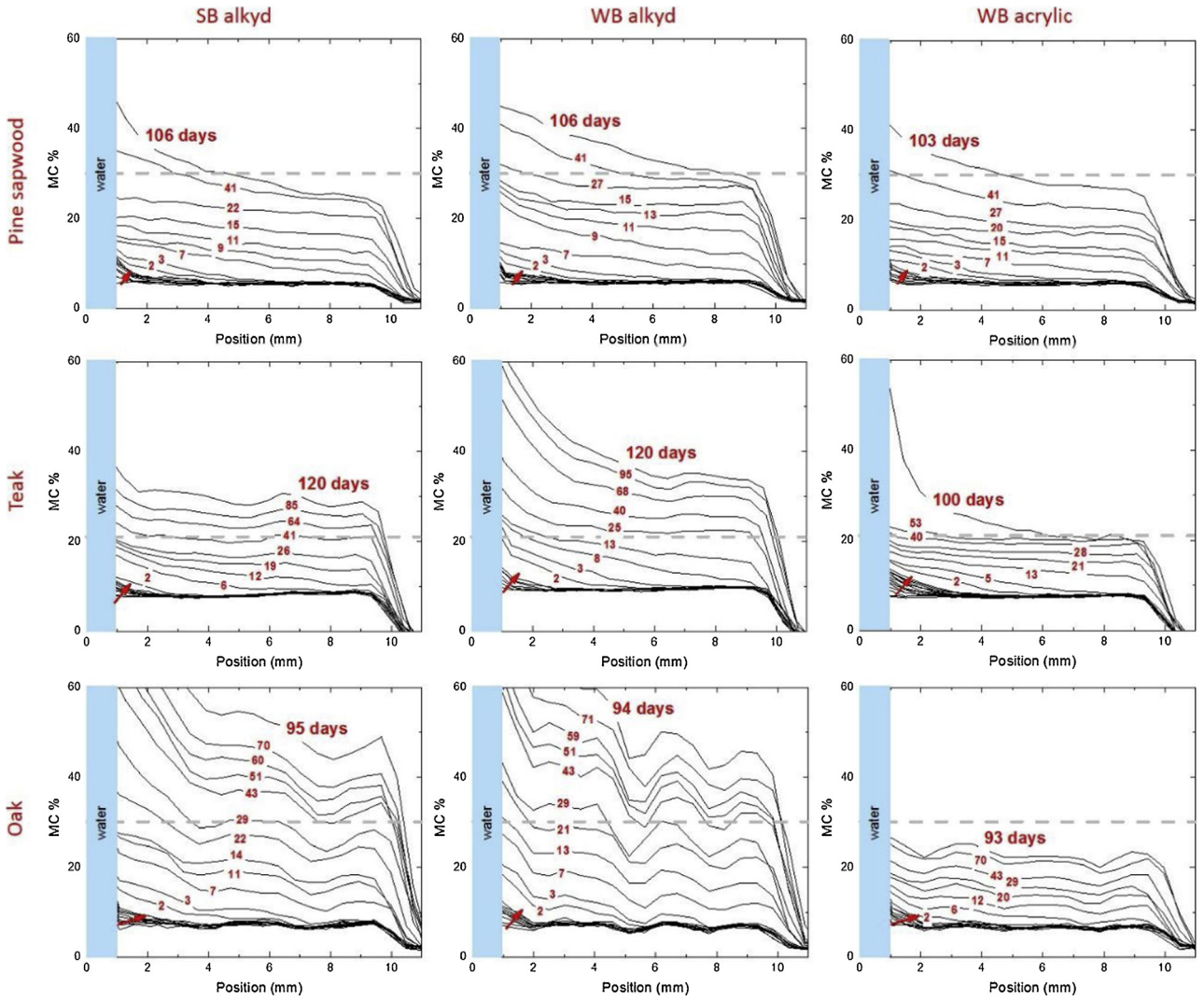

Fig. 5. The moisture content (MC) profiles of various combinations of wood (pine sapwood, teak and oak) and coating (SB alkyd, WB alkyd and WB acrylic) types during water uptake. Profiles were obtained every 2 h during the first day represented by an arrow, then at indicated times in terms of days.

third phase.

4.3. Drying after water uptake

After the liquid water uptake, drying is performed on the same samples to follow the moisture profiles during water vapour leaving the wood through the coatings. After completing long term water uptake, the remaining liquid water was taken away from the top of the samples and then the top surface was exposed to a flow of dry air. The MC profiles during drying are given in Fig. 7 for coated pine sapwood, teak and oak. The surface exposed to dry air is located at position $x = 0$. The FSP is indicated by horizontal dashed line.

In all wood-coating combinations, homogeneously decreasing profiles are observed which shows coating (externally) limited drying. Note the peak on the coated surface during the early phase of drying. This peak comes from the moisturized glue which was used to glue a glass tube on top of the samples to act as a water reservoir. When the glue is wet, it also gives NMR signal resulting the observed peak. However, it dries in time and its relaxation becomes very short that cannot give signal anymore.

The change in average MC over the whole sample during water uptake and subsequent drying is also shown in Fig. 8. The average MC has been calculated by summing up the MC values and dividing by the number of points on the MC profiles. The error bar represents the standard deviation in MC over a MC profile. Note that the average MC was calculated after the peak from moisturized glue disappears, such as 5 days after in the case of SB alkyd coated pine sapwood (see Fig. 7).

Note that the average MC below the FSP during drying will be used to calculate water permeability below the FSP.

4.4. Permeability of coatings

4.4.1. Theory

The water permeability of transparent coatings on wood can be calculated from the NMR profiles. In order to calculate permeability of coatings on wood during liquid water uptake and subsequent drying below the FSP, we performed following derivations.

The total amount of water in the wood can be connected with the flux through coating via the mass conservation equation:

$$\frac{1}{A \cdot M}\frac{\Delta m}{\Delta t} = -J \equiv -k\frac{\Delta a}{L} \tag{2}$$

where A [m^2] is the area of the coated surface exposed to liquid water or dry air and $M = 18$ g/mol is the molar mass of water. $^{\Delta m}/_{\Delta t}$ is the mass change over time. m is the total amount of water in the wood, which is obtained by multiplying θ (m/m_{wood} [g/g]) by the dry mass of the wood sample, m_{wood}.

The right side of the equation represents the flux through coating, J

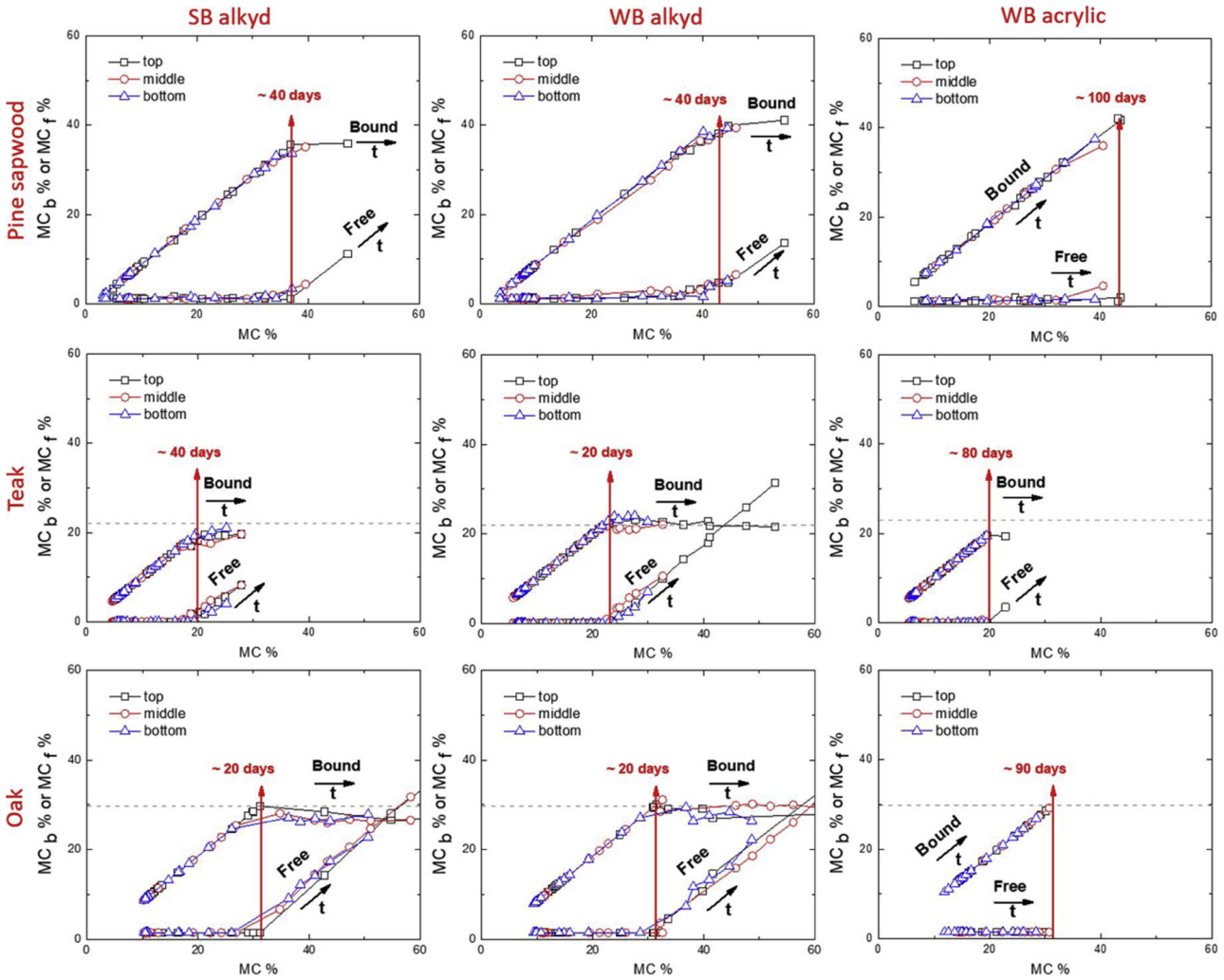

Fig. 6. Moisture contents of bound (MC_b %) and free (MC_f %) water versus total MC at 3 positions; around 2 mm (top), 5 mm (middle) and 8 mm (bottom) below the coated surface.

[g/m^{2}s]. $k \equiv D\rho$ is the permeability of the film, where D [m^2/s] is the diffusivity of water through the coating, ρ [g/m^3] is the solubility. L [m] is the thickness of the film. The driving force for the flux is the water activity difference, Δa, which is the subtraction of the water activity of the environment from the water activity of the wood.

4.5. Local flux

At a given point in the coating with a thickness L the mass flux J equals:

$$J = -D(a)\left(\frac{\partial \rho}{\partial a}\right)\frac{\partial a}{\partial x} \equiv -f(a)\frac{\partial a}{\partial x} \tag{3}$$

where f is a combination of the local diffusion coefficient and the solubility. And in case that the diffusion coefficient varies with the water content, f can be a function of a (the local water activity). Also, $\partial\rho/\partial a$ is the derivative of the sorption isotherm, where sorption comes into play.

We assume that the density distribution of water in the coating slowly varies compared to the flux, so the flux will be constant at every point in the coating. Therefore:

$$JL = -\int_0^L f(a)\frac{\partial a}{\partial x}dx = -[F(a_L) - F(a_0)] \tag{4}$$

where F is the primitive of f. When x is equal to 0, it is the coating-wood interface, so one can consider a_0 as the water activity in the wood. When x is equal to L, it is the coating-environment (like **air** in the drying process or **water** in the uptake process) interface, so a_L can be considered as the water activity of the environment. As a consequence, one can define a permeability k as,

$$k \equiv \frac{|J|\ L}{|\Delta a|} = \frac{F(a_L) - F(a_0)}{|a_L - a_0|} \tag{5}$$

4.6. Activity dependent permeability

To understand the relation between the permeability and the activities at both sides of the coating, we start with the following expression for f,

$$f(a) = f_0 + f_1 a + O(2) \tag{6}$$

The primitive of this expression (Eq. (6)) is

$$F(a) = const + f_0 a + \frac{1}{2}f_1 a^2 + O(3) \tag{7}$$

Inserting this expression (Eq. (7)) into the derived equation for the permeability (Eq. (5)) gives

$$k = \frac{F(a_L) - F(a_0)}{|a_L - a_0|} = f_0 + \frac{1}{2}f_1(a_0 + a_L) + O(2) \tag{8}$$

This expression (Eq. (8)) demonstrates the importance of the state on both sides of the coating. The second term shows how the moisture

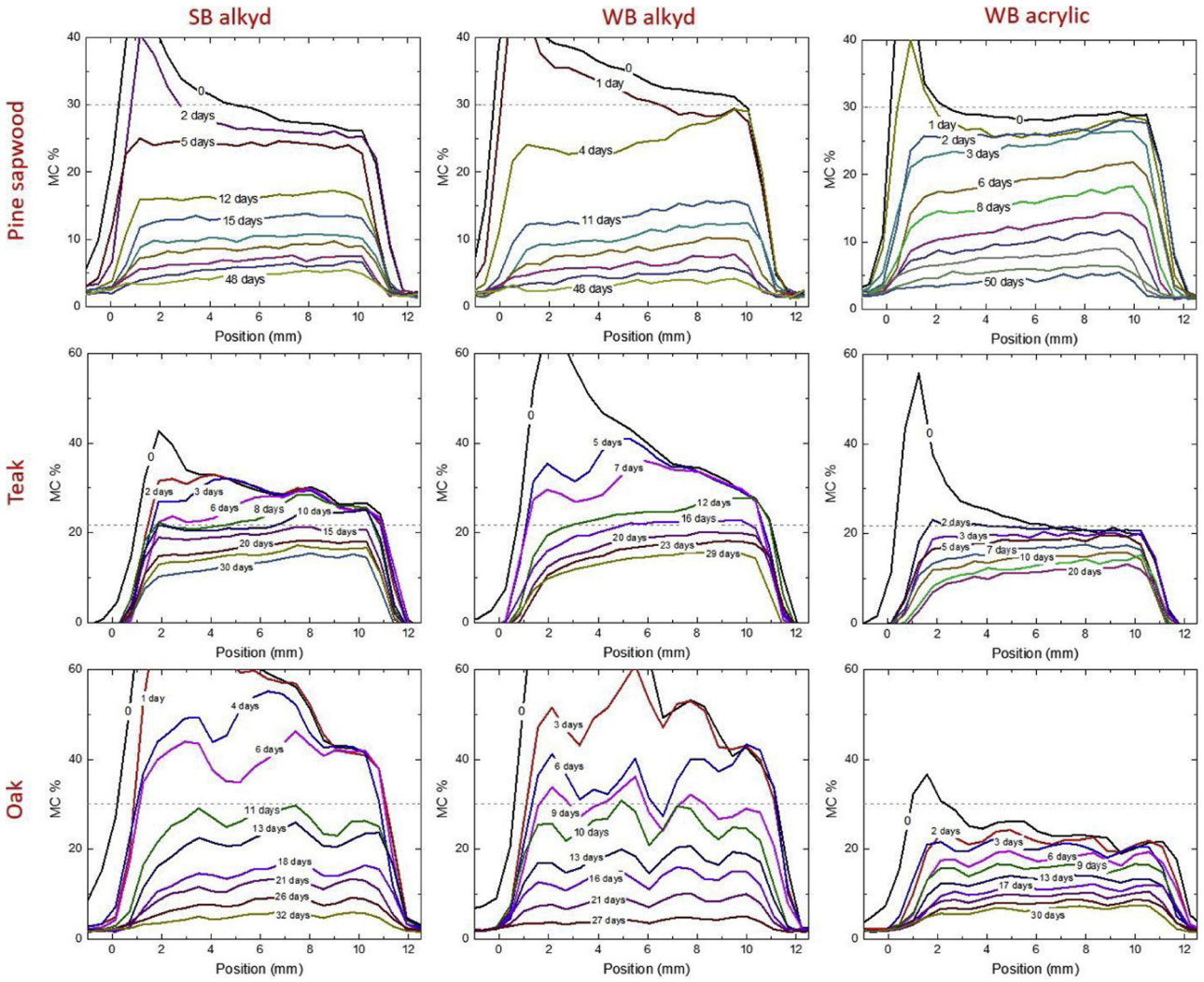

Fig. 7. The moisture content (MC) profiles of various combinations of wood (pine sapwood, teak and oak) and coating (SB alkyd, WB alkyd and WB acrylic) types during drying just after water uptake. Profiles were obtained at indicated times.

distribution in the coating could affect the permeability. It also supplies a simple parameter for this: $\frac{1}{2}(a_0 + a_L)$, which is the average water activity in the coating.

4.6.1. Permeability of one coated system

The NMR moisture profiles were used to determine the water permeability of coatings on wood by Eq. (2). WB acrylic coated pine sapwood was chosen to show how to calculate water activity dependent permeability, and its correlation with the average water activity in the coating.

Eq. (2) can be rewritten as,

$$k \equiv \frac{L}{A \cdot M} \frac{\Delta m}{\Delta t} \frac{1}{|\Delta a|} \tag{9}$$

The MC versus time graphs (Fig. 8) provides the mass change over time, $^{\Delta m}/_{\Delta t}$. Firstly, θ is multiplied by the mass of dry wood to obtain the total amount of water in the wood. Secondly, an equation is obtained for the mass change over time, which is the derivation of the fitted equation of m versus t plot (Fig. 9, left). Thirdly, θ is not constant, but depends on the water activity, $\theta(a)$. The sorption isotherms of uncoated wood in Fig. 1 are used to obtain the reverse isotherm (Fig. 9, right). The water activity in the wood is obtained at each θ value by a versus θ in Fig. 9, right.

Then the water activity difference is calculated with the value of the water activity of the environment is *1* for uptake and *0* for drying. Finally, *L*, *A* and *M* are known values, which are directly put in Eq. (9) to find permeability, see Fig. 10.

Recalling the previous section that the activities at both sides of the coating, i.e. the average water activity in the coating, could affect the permeability. Fig. 10 shows the permeability versus the average water activity in the coating for WB acrylic on pine sapwood. The average water activity of the coating is calculated by taking the average of the external water activity (*1* for uptake and *0* for drying) and the water activity inside the wood.

There are two parts in the curve; drying and uptake. There is roughly continuous curve from drying branch to uptake branch. First part, where the average water activity in the coating is below *0.5*, shows the permeability variations during drying below FSP. In this part, the permeability drops as the average water activity in the coating decreases. Second part, where the average water activity in the coating is above *0.5*, shows the permeability variations during uptake. In this part, the permeability rises as the average water activity in the coating increases. At the end of the uptake, it has the highest permeability, where the activity is *1* on both sides of the coating.

It has been observed that permeability varies as a function of average water activity, which hints towards the importance of the amount of water present inside the coating, so the sorption isotherm. In order to check if there is any correlation between the permeability and the sorption isotherm, the adsorption and desorption isotherms of

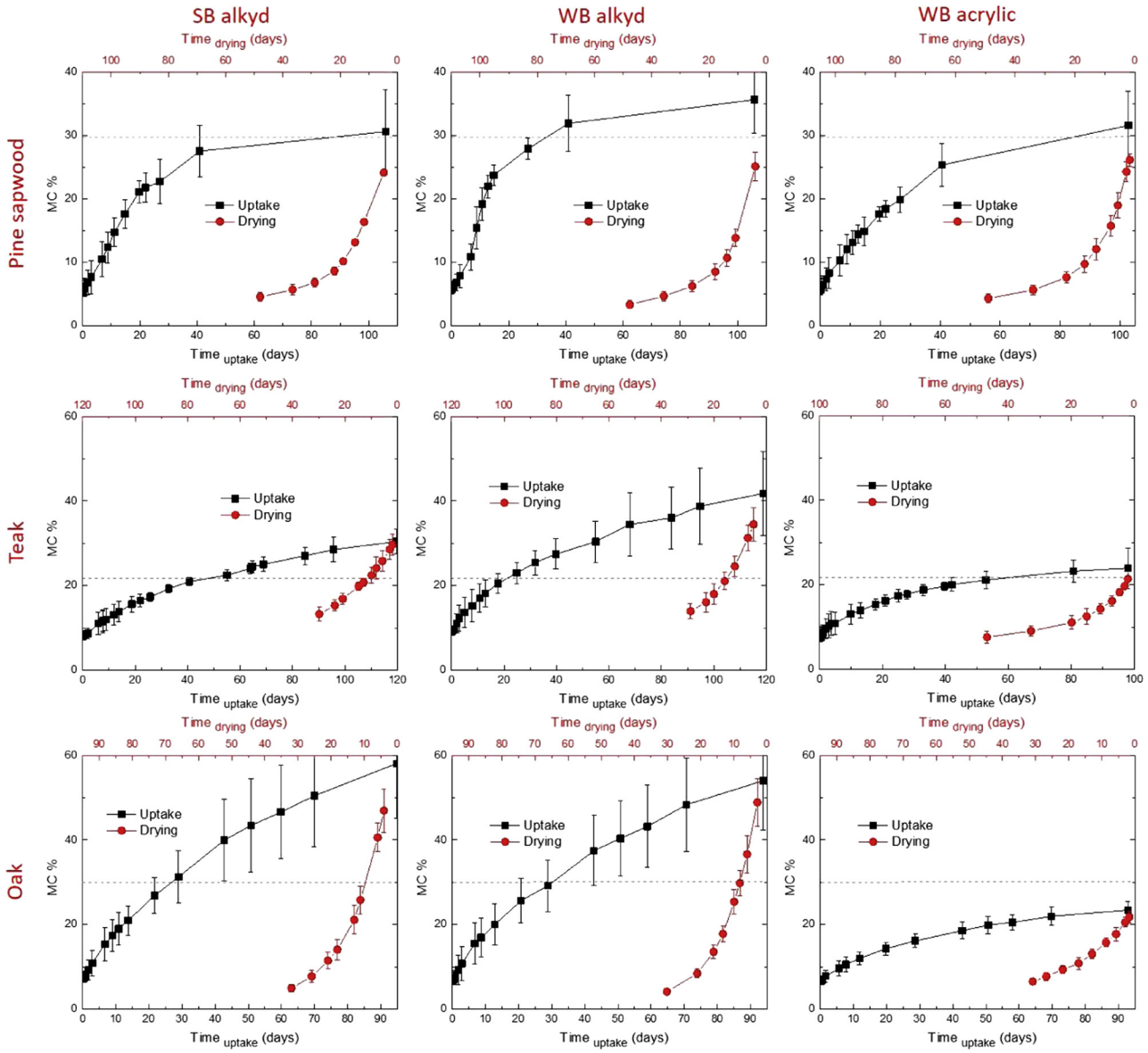

Fig. 8. The change in **average** MC over the whole sample during water uptake and subsequent drying.

leached free film for WB acrylic are shown in Fig. 10. The scale of the sorption curves is set such that it covers the scale of permeability to be able to correlate the permeability to sorption isotherms of the coating.

The trend in the permeability variations is in line with the sorption isotherms of the coating, which shows a reasonable correlation. This also proves that the permeability variations are due to the coating absorption itself. Moreover, the permeability is equal to diffusion coefficient (D) times the solubility (ρ), so the sorption isotherm basically. The good correlation of the permeability with the sorption isotherm raises the question about constant diffusion, which is an open discussion that deserves more study.

4.6.2. Permeability of all coating-wood combinations

In order to understand if the activity dependent permeability is

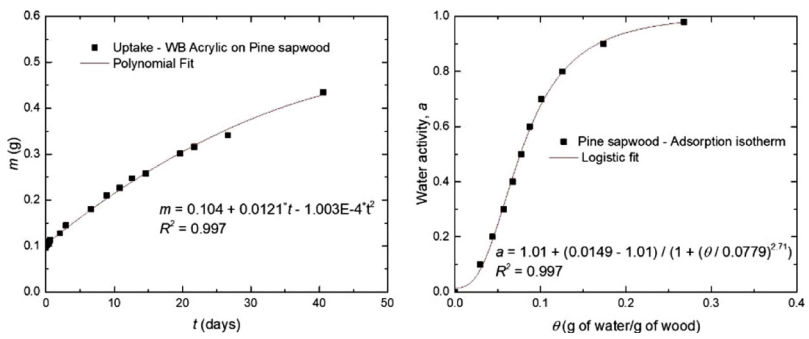

Fig. 9. Left: The total amount of water in the wood (m) versus time (t) for WB acrylic coated pine sapwood. Right: Water activity (a) versus the average moisture content (θ) for pine sapwood only.

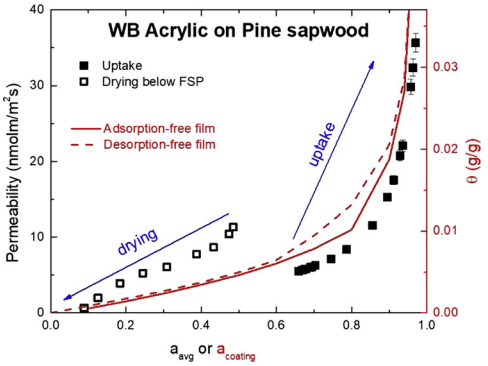

Fig. 10. Permeability of WB acrylic on pine sapwood for liquid water uptake and subsequent drying below the FSP. Adsorption and desorption isotherms of leached free films, measured by DVS were obtained from the previous study [11].

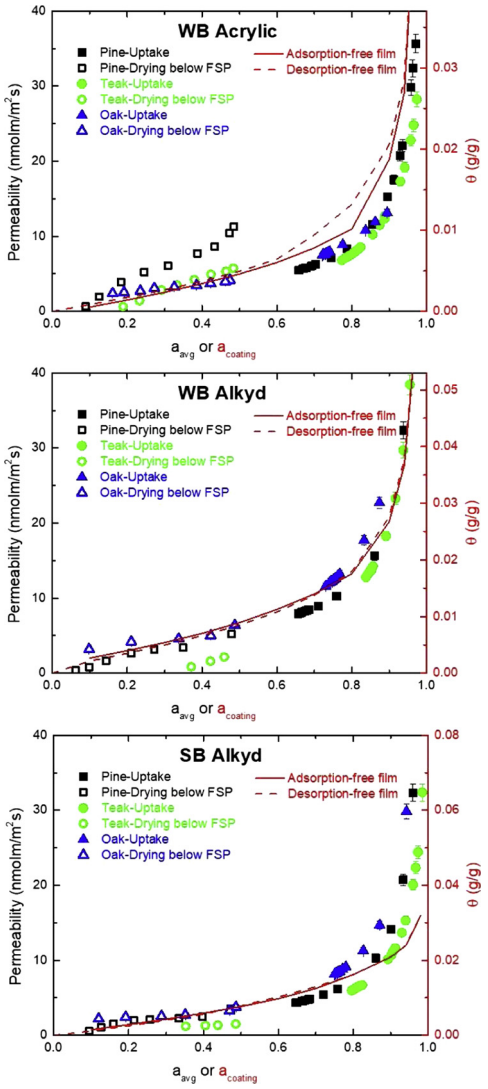

Fig. 11. Permeability of coatings (WB acrylic, WB alkyd, SB alkyd) on wood (pine, teak, oak) for liquid water uptake and subsequent drying below the FSP. Adsorption and desorption isotherms of leached free films, measured by DVS were obtained from the previous study [11].

specific for one particular system (WB acrylic on pine sapwood), or it holds for the other systems as well, the permeability variations for various combinations of wood and coating types are studied during liquid water uptake and subsequent drying, see Fig. 11.

For each coating type, there is quantitatively similar trend between different wood types. As seen in the previous study, the permeability is hardly sensitive to the wood type [11]. The permeability variations for different coating-wood combinations show the similar behaviour as the WB Acrylic on pine sapwood discussed in the previous section. Firstly, all the curves are continuous in such a way that the drying branch and the uptake branch can be easily connected together. Secondly, the permeability rises when the average activity increases during uptake, and drops when the average activity decreases during drying. In other words, the permeability has a direct relation with the average water activity inside the coating, which is connected to the activities of both sides of the coating.

The adsorption and desorption isotherms of leached coating films are shown in Fig. 11 to check if the correlation between the permeability and the sorption isotherm holds for all studied coating and wood combinations. The overall trend in the permeability variations is in line with the sorption isotherms of the coatings. For all studied systems, this correlation between the sorption isotherm and the permeability is remarkably well, suggesting that the permeability variations are due to the amount of water present in the coating. However, there is one remark that this correlation with the sorption isotherm may vary in case a polymer plasticizes above certain moisture content. This type of condition may significantly influence the permeability. Further tests are needed to check whether or not the correlation with the sorption isotherm is polymer specific. These tests should focus on polymers which can be easily plasticized. Although it is not very interesting from coating perspective, nylon could be a nice testing polymer to investigate the limitations.

The permeability variation due to the amount of water present in the coating hints towards the importance of the boundary conditions. The biggest variation in the permeability is observed at the switch from drying to uptake, where there is more water during uptake than drying. It suggests that it is not so much due to the fact that is vapour or liquid. In fact, the dependence of the permeability to physical state of water is still in debate [19–23]. As shown in this study, it is not about the type of water vapour or liquid present at one side of the coating; it is all about the moisture content of the coating which is connected to the water activities of the sides of the coating. In other words, permeability is all about the local moisture content in the coating. At this point, there is an open discussion related to the previous work [11], in which the permeability of free films was found constant via wet-cup experiments. We still have to investigate how the outcomes of this study link to the previous results found by wet-cup. This will require a more detailed series of experiments.

5. Conclusions

During both water uptake and subsequent drying studied by NMR imaging, coating limited transport is observed for the studied wood-coating combinations – three unpigmented coatings, SB alkyd, WB alkyd and WB acrylic on pine sapwood, teak and oak. During water uptake, free water is only observed after all the cell walls are saturated by the bound water, which shows a local thermodynamic equilibrium of bound and free water.

The water permeability of coatings on wood has a direct relation with the average water activity inside the coating, which is connected to the activities of both sides of the coating. The permeability rises when the average activity increases during uptake, and drops when the average activity decreases during drying. Further, the correlation between the sorption isotherms and the permeability is remarkably good, which indicates that the permeability variations are due to the amount of water present in the coating. This good correlation raises the question about constant diffusion, which is an open discussion that deserves more study. In overall, the permeability is not about the type of water vapour or liquid present at one side of the coating; it is all about the

moisture content of the coating.

A few issues upon these conclusions are needed to be addressed in future research. Further tests are suggested to check whether or not the correlation between the permeability and the sorption isotherm is polymer specific. This requires a study on easily plasticized polymers in which nylon could be a nice testing polymer to investigate the limitations. Secondly, it has to be still investigated how wet-cup experiments fit in the outcomes of this study that requires a more detailed series of experiments, such as more points in the dry region.

Acknowledgements

The research is funded by AkzoNobel Decorative Paints. The authors would like to thank Paul van de Keer and AkzoNobel Analytical Services Sassenheim for optical microscope images; Hans Dalderop and Jef Noijen from TU/e for their technical support; Joldert Faber, Francis Duivenvoorde and Anthonie Stuiver from AkzoNobel for useful discussions.

References

[1] A.J. Stamm, Review of nine methods for determining the fiber saturation points of wood and wood products, Wood Sci. 4 (1971) 114–128.
[2] P. Ahola, H. Derbyshire, G. Hora, M. de Meijer, Water protection of wooden window joinery painted with low organic solvent content paints with known composition. Part 1. Results of inter-laboratory tests, Holz Als Roh- Und Werkst 57 (1999) 45–50, https://doi.org/10.1007/PL00002620.
[3] J. Ekstedt, G. Östberg, Liquid water permeability of exterior wood coatings-testing according to a proposed european standard method, J. Coat. Technol. Res. 73 (2001) 53–59, https://doi.org/10.1007/BF02698438.
[4] J. Ekstedt, Influence of coating system composition on moisture dynamic performance of coated wood, J. Coat. Technol. Res. 75 (2003) 27–37, https://doi.org/10.1007/BF02697719.
[5] S.V. Dvinskikh, M. Henriksson, A.L. Mendicino, S. Fortino, T. Toratti, NMR imaging study and multi-Fickian numerical simulation of moisture transfer in Norway spruce samples, Eng. Struct. 33 (2011) 3079–3086, https://doi.org/10.1016/j.engstruct.2011.04.011.
[6] P. Pourmand, L. Wang, S.V. Dvinskikh, Assessment of moisture protective properties of wood coatings by a portable NMR sensor, J. Coatings Technol. Res. 8 (2011) 649–654, https://doi.org/10.1007/s11998-011-9348-8.
[7] P.A. van Meel, S.J.F. Erich, H.P. Huinink, K. Kopinga, J. de Jong, O.C.G. Adan, Moisture transport in coated wood, Prog. Org. Coatings. 72 (2011) 686–694, https://doi.org/10.1016/j.porgcoat.2011.07.011.
[8] J. Johansson, Å. Blom, S. Dvinskikh, NMR-measurements for determination of local moisture content of coated wood, J. Coat. Technol. Res. 10 (2013) 601–607, https://doi.org/10.1007/s11998-013-9484-4.
[9] V. Bucur, Nondestructive Characterization and Imaging of Wood, Springer, Berlin Heidelberg, 2003.
[10] Ö. Gezici-Koç, S.J.F. Erich, H.P. Huinink, L.G.J. van der Ven, O.C.G. Adan, Bound and free water distribution in wood during water uptake and drying as measured by 1D magnetic resonance imaging, Cellulose 24 (2017) 535–553, https://doi.org/10.1007/s10570-016-1173-x.
[11] Ö. Gezici-Koç, S.J.F. Erich, H.P. Huinink, L.G.J. van der Ven, O.C.G. Adan, Understanding the influence of wood as a substrate on the permeability of coatings by NMR imaging and wet-cup, Prog. Org. Coat. 114 (2018) 135–144, https://doi.org/10.1016/j.porgcoat.2017.10.013.
[12] P.A.J. Donkers, H.P. Huinink, S.J.F. Erich, N.J.W. Reuvers, O.C.G. Adan, Water permeability of pigmented waterborne coatings, Prog. Org. Coat. 76 (2013) 60–69, https://doi.org/10.1016/j.porgcoat.2012.08.011.
[13] P. Wiberg, S.M.B. Sehlstedt-P, T.J. Morén, Heat and mass transfer during sapwood drying above the fibre saturation point, Dry. Technol. 18 (2000) 1647–1664, https://doi.org/10.1080/07373930008917804.
[14] M. de Meijer, H. Militz, Moisture transport in coated wood. Part 1: analysis of sorption rates and moisture content profiles in spruce during liquid water uptake, Holz Als Roh- Und Werkst 58 (2000) 354–362, https://doi.org/10.1007/s001070050445.
[15] K. Sandberg, J.-G. Salin, Liquid water absorption in dried Norway spruce timber measured with CT scanning and viewed as a percolation process, Wood Sci. Technol. 46 (2010) 207–219, https://doi.org/10.1007/s00226-010-0371-1.
[16] W. Sonderegger, M. Glaunsinger, D. Mannes, T. Volkmer, P. Niemz, Investigations into the influence of two different wood coatings on water diffusion determined by means of neutron imaging, Eur. J. Wood Wood Prod. (2015), https://doi.org/10.1007/s00107-015-0951-8.
[17] M. Sedighi-Gilani, M. Griffa, D. Mannes, E. Lehmann, J. Carmeliet, D. Derome, Visualization and quantification of liquid water transport in softwood by means of neutron radiography, Int. J. Heat Mass Transf. 55 (2012) 6211–6221, https://doi.org/10.1016/j.ijheatmasstransfer.2012.06.045.
[18] D. Topgaard, O. Söderman, Changes of cellulose fiber wall structure during drying investigated using NMR self-diffusion and relaxation experiments, Cellulose 9 (2002) 139–147, https://doi.org/10.1023/A:1020158524621.
[19] N.S. Sangaj, V.C. Malshe, Permeability of polymers in protective organic coatings, Prog. Org. Coat. 50 (2004) 28–39, https://doi.org/10.1016/j.porgcoat.2003.09.015.
[20] J. Graystone, Moisture transport through wood coatings: the unanswered questions, Surf. Coat. Int. Part B Coat. Trans. 84 (2001) 177–187, https://doi.org/10.1007/BF02700396.
[21] M. Huldén, C.M. Hansen, Water permeation in coatings, Prog. Org. Coat. 13 (1985) 171–194, https://doi.org/10.1016/0033-0655(85)80025-X.
[22] G.K. van der Wel, O.C.G. Adan, Moisture in organic coatings — a review, Prog. Org. Coat. 37 (1999) 1–14, https://doi.org/10.1016/S0300-9440(99)00058-2.
[23] J. Sivadjian, D. Ribeiro, Comparative studies on the permeability to water and to water vapor of plastic materials by the hygrophotographic technique, J. Appl. Polym. Sci. 8 (1964) 1403–1413, https://doi.org/10.1002/app.1964.070080330.
[24] N. Agarwal, R.J. Farris, Water absorption by acrylic-based latex blend films and its effect on their properties, J. Appl. Polym. Sci. 72 (1999) 1407–1419 doi:10.1002/(SICI)1097-4628(19990613)72:11 < 1407::AID-APP4 > 3.0.CO;2-5.
[25] B. Jiang, J.G. Tsavalas, D.C. Sundberg, Water whitening of polymer films: mechanistic studies and comparisons between water and solvent borne films, Prog. Org. Coat. 105 (2017) 56–66, https://doi.org/10.1016/j.porgcoat.2016.12.027.
[26] ISO 2808:2007 Paints and varnishes – determination of film thickness, (n.d.). https://www.iso.org/standard/37486.html.
[27] ISO 1463:2003 Metallic and oxide coatings – measurement of coating thickness – microscopical method, (n.d.). https://www.iso.org/standard/31239.html.
[28] Ö. Gezici-Koç, C.A.A.M. Thomas, M.-E.B. Michel, S.J.F. Erich, H.P. Huinink, J. Flapper, F.L. Duivenvoorde, L.G.J. van der Ven, O.C.G. Adan, In-depth study of drying solvent-borne alkyd coatings in presence of Mn- and Fe- based catalysts as cobalt alternatives, Mater. Today Commun. 7 (2016) 22–31, https://doi.org/10.1016/j.mtcomm.2016.03.001.
[29] S.J.F. Erich, Ö. Gezici-Koç, M.-E.B. Michel, C.A.A.M. Thomas, L.G.J. van der Ven, H.P. Huinink, J. Flapper, F.L. Duivenvoorde, O.C.G. Adan, The influence of calcium and zirconium based secondary driers on drying solvent borne alkyd coatings, Polymer 121 (2017) 262–273, https://doi.org/10.1016/j.polymer.2017.06.031.
[30] V.V. Telkki, M. Yliniemi, J. Jokisaari, Moisture in softwoods: fiber saturation point, hydroxyl site content, and the amount of micropores as determined from NMR relaxation time distributions, Holzforschung 67 (2013) 291–300, https://doi.org/10.1515/hf-2012-0057.
[31] C.A.S. Hill, The reduction in the fibre saturation point of wood due to chemical modification using anhydride reagents: a reappraisal, Holzforschung 62 (2008) 423, https://doi.org/10.1515/HF.2008.078.
[32] T. Arends, L. Pel, H.P. Huinink, Hygromorphic response dynamics of oak: towards accelerated material characterization, Mater. Struct. 50 (2017) 181, https://doi.org/10.1617/s11527-017-1043-5.